

# Prostate-Specific Antigen Is a “Chymotrypsin-like” Serine Protease with Unique P1 Substrate Specificity<sup>†</sup>

Aaron M. LeBeau,<sup>‡,§</sup> Pratap Singh,<sup>§,||</sup> John T. Isaacs,<sup>§,||</sup> and Samuel R. Denmeade<sup>\*,‡,§,||</sup>

Department of Pharmacology and Molecular Sciences, The Sidney Kimmel Comprehensive Cancer Center at Johns Hopkins, and Department of Chemical and Biomolecular Engineering, The Johns Hopkins University, Baltimore, Maryland 21231

Received February 4, 2009; Revised Manuscript Received March 12, 2009

**ABSTRACT:** Prostate-specific antigen (PSA), a serine protease belonging to the human kallikrein family, is best known as a prostate cancer biomarker. Emerging evidence suggests that PSA may also play a salient role in prostate cancer development and progression. With large amounts of enzymatically active PSA continuously and selectively produced by all stages of prostate cancer, PSA is an attractive target. PSA inhibitors, therefore, may represent a promising class of therapeutics and/or imaging agents. PSA displays chymotrypsin-like specificity, cleaving after hydrophobic residues, in addition to possessing a unique ability to cleave after glutamine in the P1 position. In this study, we investigated the structural motifs of the PSA S1 pocket that give it a distinct architecture and specificity when compared to the S1 pocket of chymotrypsin. Using the previously described PSA substrate Ser-Ser-Lys-Leu-Gln (SSKLQ) as a template, peptide aldehyde based inhibitors containing novel P1 aldehydes were made and tested against both proteases. Glutamine derivative aldehydes were highly specific for PSA while inhibitors with hydrophobic P1 aldehydes were potent inhibitors of both proteases with  $K_i$  values <500 nM. The crystal structure of PSA was used to generate a model that allowed GOLD docking studies to be performed to further understand the critical interactions required for inhibitor binding to the S1 pockets of PSA and chymotrypsin. In conclusion, these results provide experimental and structural evidence that the S1 specificity pocket of PSA is distinctly different from that of chymotrypsin and that the development of highly specific PSA inhibitors is feasible.

Prostate-specific antigen (PSA)<sup>1</sup> is a member of the kallikrein family of serine proteases where it is known as kallikrein-related peptidase 3 (KLK3). The expression of PSA is highly restricted to normal and malignant prostate epithelial cells in men, and for this reason, PSA is used extensively as a biomarker to screen for prostate cancer, to detect recurrence after definitive therapy, and to follow response to treatment in the metastatic disease setting (1, 2). The major physiologic substrates for PSA appear to be the gel-forming proteins in freshly ejaculated semen, semenogelin I (SgI) and semenogelin II (SgII) which are synthesized and secreted by the seminal vesicles (3–5). Active PSA in the seminal fluid cleaves preferentially after tyrosyl and glutaminyl peptide bonds to generate multiple soluble

fragments of SgI and SgII (3, 4). PSA can also cleave a number of growth regulatory proteins that are important in cancer growth and survival. These include insulin growth factor binding proteins (IGFBP) 2, 3, and 5 (6), PTH-related protein (7, 8), latent TGF- $\beta$ 2 (9), and extracellular matrix components fibronectin and laminin (10). The exclusive production of PSA by prostate cancers, coupled with evidence of PSA's role in prostate cancer progression, suggests that PSA inhibition may represent a novel therapeutic strategy for the treatment of prostate cancer.

Whereas most of the other kallikreins have trypsin-like proteolytic activity (1, 2), PSA is considered a chymotrypsin-like protease based on similarities with chymotrypsin in the S1 specificity pocket of the catalytic site and its preference for cleaving after hydrophobic residues in the P1 position. While PSA has some similarity to chymotrypsin in its preference for amino acids at the P1 position, PSA also displays enzymatic properties that differentiate it from chymotrypsin and other serine proteases. These differences suggest that there may be highly specific protein substrates for PSA that are not yet identified. While a number of bacterial and viral proteases can cleave after glutamine, PSA is one of the few known mammalian serine proteases that can cleave after glutamine residues present in a known physiologic substrate (i.e., SgI and SgII) (5, 11, 12). PSA cleavage sites within SgI and SgII have been mapped, and of the 29 mapped sites, ~40% contain Gln in the P1 position (4, 5). Although PSA, like chymotrypsin, can cleave

<sup>†</sup> This work was supported by a Prostate SPORE grant (P50CA58236) to J.T.I. and S.R.D. and a grant from the One-in-Six Foundation, Akron, OH, to S.R.D.

\* Address correspondence to this author. Phone: 410-502-3941. Fax: 410-614-8397. E-mail: denmesa@jhmi.edu.

<sup>‡</sup> Department of Pharmacology and Molecular Sciences, The Johns Hopkins University.

<sup>§</sup> The Sidney Kimmel Comprehensive Cancer Center at Johns Hopkins, The Johns Hopkins University.

<sup>||</sup> Department of Chemical and Biomolecular Engineering, The Johns Hopkins University.

<sup>1</sup> Abbreviations: PSA, prostate-specific antigen; Sg, semenogelin; IGFBP, insulin growth factor binding protein; PTHrP, parathyroid related protein; TGF- $\beta$ 2, transforming growth factor  $\beta$ 2; ACT,  $\alpha$ 1-antichymotrypsin; TPCK, tosylphenylalanine chloromethyl ketone; PMSF, phenylmethanesulfonyl fluoride; Fmoc, 9-fluorenylmethyl chloroformate; Cbz, benzyloxycarbonyl;  $K_i$ , inhibition constant.

the Leu<sup>358</sup>-Ser<sup>359</sup> linkage within the serum protease inhibitor  $\alpha$ 1-antichymotrypsin (ACT) to form a stable complex, the classic chymotrypsin inhibitors tosylphenylalanine chloromethyl ketone (TPCK) and phenylmethanesulfonyl fluoride (PMSF) are poor PSA inhibitors. PSA is also not inhibited well by the panel of protease inhibitors present in commercially available protease inhibitory cocktails such as Complete protease inhibitor (unpublished data).

These combined results suggest that PSA has unique substrate requirements compared to chymotrypsin that would allow for the development of highly specific inhibitors of PSA's proteolytic activity. In this study to generate PSA specific inhibitors, peptide aldehyde inhibitors and molecular modeling were used to identify the structural differences between PSA and chymotrypsin in the S1 pocket that underlie their differences in substrate recognition. To evaluate these differences, we used a previously described PSA specific substrate with the sequence Ser-Ser-Lys-Leu-Gln (SSKLQ) (13), generated from the semenogelin cleavage map, as the template for generating the peptide aldehyde based inhibitors of PSA. To probe differences in substrate recognition, we focused on the S1 subsite which determines the characteristic specificity of the protease. We generated peptide aldehydes using the SSKL-X template, substituting naturally and unnaturally occurring amino acids in the P1 position and compared their ability to inhibit PSA and chymotrypsin. Molecular models of the S1 subsite for both PSA and chymotrypsin were generated, based on previously published crystal structures, in order to evaluate the key interactions between P1 side chains and the specific amino acids lining the S1 pocket. The overarching goal of this study was to gain structural insights into the P1 specificity of PSA and determine salient structural motifs that could then be used for the further design of more potent and specific peptide (boronic acids, chloromethyl ketones) and nonpeptide based inhibitors that could be used to develop targeted therapeutics and imaging agents for the treatment and detection of prostate cancer.

## MATERIALS AND METHODS

**Materials.** PSA was purchased from Calbiochem (San Diego, CA). The fluorescent PSA substrate, morpholinocarbonyl-Ser-Arg-Lys-Gln-Gln-Tyr-aminomethylcoumarin (MuSRKSQQY-AMC), was selected as the PSA substrate based on a previous characterization study (13, 14) and was custom synthesized by California Peptides (Napa Valley, CA). Bovine  $\alpha$ -chymotrypsin and the chymotrypsin substrate, *N*-succinyl-Ala-Ala-Phe-aminomethylcoumarin (Suc-AAF-AMC), were purchased from Sigma-Aldrich (St. Louis, MO). All Fmoc amino acids used in standard Fmoc solid-phase peptide synthesis were purchased from AnaSpec (San Jose, CA). Cbz-protected amino acids were purchased from Novabiochem (San Diego, CA). Unless noted, all other reagents were from Sigma-Aldrich (St. Louis, MO).

**Peptide Aldehyde Synthesis.** Compounds **1–3**, **9**, **10**, **12**, and **15–17** were synthesized by oxidizing the corresponding Fmoc-amino alcohol to an aldehyde using IBX-PS resin (Novabiochem Tech Bulletin) and loading the resulting aldehyde onto H-Thr-Gly-NovaSyn TG resin according to the manufacturer's conditions. Fmoc solid-phase synthesis was then performed on an AAPPTec Apex 396 peptide

synthesizer. Side chain deprotection while on the H-Thr-Gly-NovaSyn TG resin was done by treating the resin with neat TFA (2  $\times$  45 min). The peptide aldehydes were cleaved from the resin using three treatments of AcOH/H<sub>2</sub>O/CH<sub>2</sub>Cl<sub>2</sub>/MeOH (10:5:64:21) for 30 min. Precursor compounds of **2** and **3** were synthesized as previously described by Malcolm et al. (15), compounds **4–8** and **11** were synthesized as described by Webber et al. (16), and compounds **13** and **14** were synthesized as described previously (14, 17). The peptide aldehydes were characterized using mass spectrometry (Bruker 3000 Esquire ESI) and NMR (400 MHz Bruker Ultrashield) and were HPLC purified on a Waters Delta 600 semiprep system using a Phenomenex Luna 10u C18 250  $\times$  10 mm semiprep column. The HPLC gradient profile was linear starting at 100% solvent A (0.1% TFA in H<sub>2</sub>O) and changing to 100% solvent B (0.1% TFA in acetonitrile) over 25 min with a flow rate of 8 mL/min. For additional information see the Supporting Information.

**Enzymatic Assays and Inhibition Kinetics.** The assay for PSA activity was performed as previously described (17, 18). The PSA concentration per assay was 2.5  $\mu$ g/mL (2 nM active PSA) with a PSA substrate concentration of 300  $\mu$ M. Substrate hydrolysis  $\pm$  inhibitor over a range of concentrations was monitored by measuring fluorescence change secondary to AMC release. Complete hydrolysis of the substrate was maintained below 5% to ensure that the substrate concentration was essentially constant. The inhibition constant values were determined using the method of progress curves of Nagase and Salvesen (19) as previously described (14). To assess inhibitor specificity, chymotrypsin (2 nM) was assayed with 25  $\mu$ M suc-AAF-AMC in the presence or absence of inhibitor over a range of concentrations.

**Molecular Modeling and Docking.** The recently solved crystal structure of PSA in complex with a substrate acyl-enzyme intermediate (PDB code 2ZCK) (20) was obtained from the RCSB Protein Data Bank and prepared for molecular modeling analysis using the MOE modeling package (CCG, Montreal, Canada). The Fab antibody fragment and one of the protein chains in the PSA dimer was removed in order to extract a single molecule of PSA enzyme in complex with the peptide substrate. Furthermore, the peptide substrate, crystallographic water molecules, and the carbohydrate side chain at Asn<sup>62</sup> residue were deleted, resulting in a PSA molecule with an empty catalytic pocket. Subsequently, hydrogens were added to the heavy atoms, and the residues were assigned the appropriate protonation states at pH 7.4. Specifically, the histidine residues were kept in a singly protonated state at N $\epsilon$ 1. The catalytic Ser<sup>195</sup> residue was deprotonated to mimic the covalent acyl-enzyme conformation as observed in the crystal structure. The resulting PSA molecule was saved in a Tripos MOL2 format and transported to GOLD software (CCDC, Cambridge, U.K.) for subsequent docking calculations.

The  $\alpha$ -chymotrypsin molecule was prepared similarly using the crystal structure (PDB code 1YPH) obtained from the RCSB Protein Data Bank. The resulting chymotrypsin molecule with hydrogens was saved in the MOL2 format and transported to GOLD software for subsequent docking calculations. In order to elucidate the structural and molecular differences, the final PSA and chymotrypsin molecules were structurally superposed using the Align module of the MOE software.

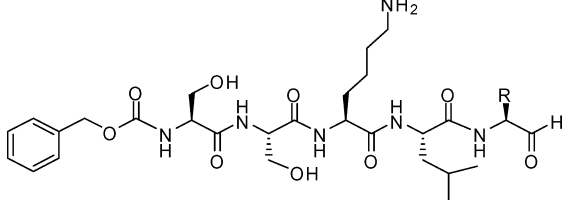
The aldehyde ligands with corresponding P1 residues were built in the MOE package using the Builder module. Partial charges were assigned using the CHARMM22 force field. The inhibitor ligands were acetylated at the N-terminus to mimic the peptide backbone of a larger peptide and to remove the artificial effects of a charged amine at the N-terminus. These ligands were energy minimized and saved in MOL2 format and transported into GOLD software for subsequent docking runs. The GOLD v3.2 program (CCDC, Cambridge, U.K.) was used to dock peptide inhibitors into the catalytic site of PSA and chymotrypsin as previously described. A scaffold constraint was used to restrict the inhibitor peptide backbone into the canonical conformation observed for the peptide substrate in the PSA and chymotrypsin crystal structure. As an internal validation of the docking methodology, the peptide substrate KGISSQY used to generate the published PSA crystal structure was redocked into the empty catalytic pocket of the all-atom PSA structure using the same docking protocols. The conformation of the top scoring pose was compared to its crystal structure conformation in order to judge the success of the docking methodology in reproducing the crystal structure confirmation.

## RESULTS

The recognition of glutamine in the P1 position of peptide substrates appears to be relatively unique to PSA. The first set of studies was designed to evaluate this specificity with glutamine containing aldehyde inhibitors using the SSKL-X template (13). The evaluation of P1 glutamine aldehyde inhibitors is problematic because the carboxamide side chain reacts with the aldehyde functional group to form a cyclic hemiaminal. While NMR analysis confirmed that the full-length glutamine aldehyde **1** was in equilibrium between a cyclic hemiaminal and an aldehyde (data not shown), it was still a modest inhibitor of PSA with a  $K_i$  of 45.21  $\mu\text{M}$  (Table 1). Although cyclization does occur and is thermodynamically favored, the side chain is still potent and able to form favorable interactions with the bottom of the S1 pocket. This suggested that a noncyclizable glutamine aldehyde derivative would be an even more potent PSA inhibitor. Thus, the noncyclizable  $\gamma$ -*N,N*-dimethylglutamine derivative **2** had a nearly 20-fold lower  $K_i$  of 2.53  $\mu\text{M}$  compared to **1**. PSA inhibitor **2** still possessed the predicted desired motif: a side chain with two hydrophobic methylenes, an amide carbonyl, and a nitrogen with a lone pair of electrons that were in the vicinity of other polar residues and could act as hydrogen bond acceptors. A decrease in the side chain length by one methylene, as in the case of  $\gamma$ -*N,N*-dimethylasparagine **3**, affected the ability of the amide group to reach down into the bottom of the S1 pocket and lead to a less potent inhibitor with a  $K_i$  of 13.09  $\mu\text{M}$  for PSA (Table 1).

The next series of inhibitors tested were the isostere replacement derivatives of glutamine. On the basis of the results with the noncyclizable derivatives **2** and **3**, this series included inhibitors whose side chain length was long enough to avoid any unfavorable interactions with the walls of the S1 pocket. With these derivatives, a pronounced increase in the ability to inhibit PSA was seen. The best compound of this series, the *N*-formyl derivative **4**, had a  $K_i$  of 0.909  $\mu\text{M}$  for PSA (Table 1). To determine whether bulkier side chains on the P1 substituent inhibitors produced steric clashes with

Table 1: Chemical Structures,  $K_i$  Values, and GOLD Scores of the PSA Inhibitors Used in This Study



compd	R	$K_i$ ( $\mu\text{M}$ ) <sup>a</sup>	GOLD score (PSA)
<b>1</b>	CH <sub>2</sub> CH <sub>2</sub> CONH <sub>2</sub>	45.21 ± 3.89	33.45
<b>2</b>	CH <sub>2</sub> CH <sub>2</sub> CON(CH <sub>3</sub> ) <sub>2</sub>	2.53 ± 0.13	30.66
<b>3</b>	CH <sub>2</sub> CON(CH <sub>3</sub> ) <sub>2</sub>	13.09 ± 0.88	19.82
<b>4</b>	CH <sub>2</sub> NHCHO	0.91 ± 0.06	29.54
<b>5</b>	CH <sub>2</sub> NHCOCH <sub>3</sub>	3.91 ± 0.35	29.56
<b>6</b>	CH <sub>2</sub> NHCOCH <sub>2</sub> CH <sub>3</sub>	9.84 ± 0.33	34.13
<b>7</b>	CH <sub>2</sub> NHCOCH(CH <sub>3</sub> ) <sub>2</sub>	13.28 ± 0.93	33.25
<b>8</b>	CH <sub>2</sub> NHCO(C <sub>6</sub> H <sub>5</sub> )	>25	27.55
<b>9</b>	CH <sub>2</sub> CH <sub>2</sub> SCH <sub>3</sub>	3.84 ± 0.21	34.77
<b>10</b>	CH <sub>2</sub> CH <sub>2</sub> SOCH <sub>3</sub>	7.25 ± 0.44	38.27
<b>11</b>	CH <sub>2</sub> CH <sub>2</sub> CN	8.14 ± 0.29	27.47
<b>12</b>	CH(CH <sub>3</sub> ) <sub>2</sub>	>100	16.16
<b>13</b>	CH <sub>2</sub> CH(CH <sub>3</sub> ) <sub>2</sub>	6.51 ± 0.25	26.37
<b>14</b>	CH <sub>2</sub> CH <sub>2</sub> CH <sub>2</sub> CH <sub>3</sub>	11.24 ± 0.26	30.93
<b>15</b>	C <sub>6</sub> H <sub>5</sub>	>100	22.92
<b>16</b>	CH <sub>2</sub> (C <sub>6</sub> H <sub>5</sub> )	0.57 ± 0.04	38.84
<b>17</b>	CH <sub>2</sub> (C <sub>6</sub> H <sub>5</sub> )OH	0.37 ± 0.02	39.66

<sup>a</sup> Value reported is for  $n = 3$  (±SE).

the walls of the S1 pocket, compounds **5**–**8** were generated. Compound **5**, with the acetyl group on the  $\gamma$ -amine, had a higher  $K_i$  of 3.91  $\mu\text{M}$ . The propyl side chain of **6** made it a less effective inhibitor than **5** with a  $K_i$  nearly three times as high. In general, the  $K_i$  values for the compounds steadily increased as the alkyl chain increased in size and branching. These data highlight the importance of the interplay between sterics and electronics in the S1 pocket.

Positional scanning studies have documented the ability of PSA to cleave after methionine residues (21). Peptide aldehydes containing a P1 methionine **9** and methionine sulfoxide **10** were able to inhibit PSA, with **9** having a lower  $K_i$  of 3.84  $\mu\text{M}$  and **10** possessing a nearly 2-fold higher  $K_i$  of 7.25  $\mu\text{M}$  (Table 1). Additionally, the glutamine aldehyde derivative **11**, in which the carboxamide of the glutamine side chain was replaced with a nitrile group that can act as a hydrogen bond acceptor, was also able to inhibit PSA ( $K_i = 8.14 \mu\text{M}$ ).

The peptide aldehydes with hydrophobic P1 aldehydes containing natural and unnatural amino acids were next tested. Compound **12**, the full-length valine aldehyde, was not an inhibitor of PSA with a  $K_i > 100 \mu\text{M}$  (Table 1). By increasing the side chain of the valine by one methylene to the leucine aldehyde **13**, the  $K_i$  decreased to 6.51  $\mu\text{M}$ , emphasizing that while  $\beta$ -branching is not well-tolerated,  $\gamma$ -branching is allowed. The norleucine aldehyde **14**, containing the longest hydrocarbon side chain out of the series, worked as an inhibitor, however, with a higher  $K_i$  of 11.24  $\mu\text{M}$ . The P1 phenylglycine aldehyde derivative **15** did not inhibit PSA with a  $K_i > 100 \mu\text{M}$ . Moving from **15** to the phenylalanine aldehyde **16**, a marked decrease in the  $K_i$  was observed yielding a submicromolar  $K_i$  of 0.57  $\mu\text{M}$  (Table 1). The substitution of a phenolic side chain as in the tyrosine aldehyde **17** produced an even more potent PSA inhibitor with a  $K_i$  of 0.37  $\mu\text{M}$  (Figure 2A).

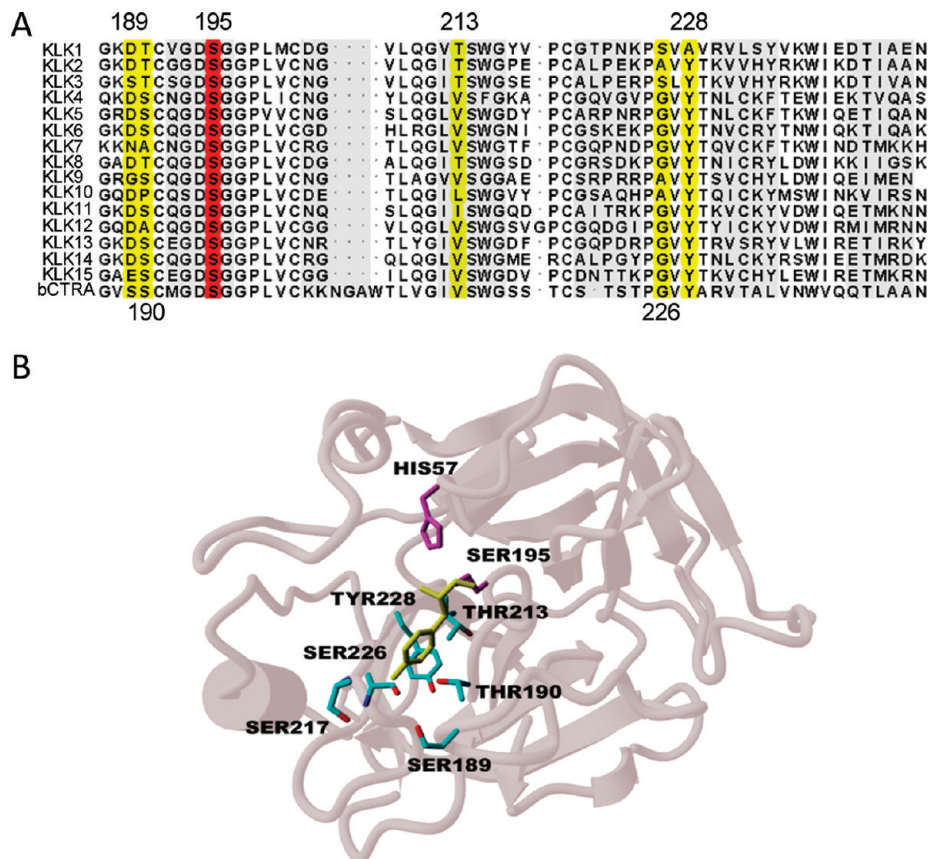


FIGURE 1: (A) Sequence alignment of the 15 human kallikreins and bovine  $\alpha$ -chymotrypsin. Only the residues spanning the S1 pocket of serine proteases are presented. The residues highlighted in yellow are critical for the P1 specificities of the respective protease. The catalytic Ser<sup>195</sup> residue is highlighted in red. (B) Ribbon representation of the S1 specificity pocket of prostate-specific antigen. The protease residues lining the pocket are shown in cyan while the catalytic histidine and serine residues are shown in magenta. The S1 tyrosine residue of peptide substrate KGISSQY is shown in yellow.

**Structural Features of the S1 Pocket of PSA.** The sequence alignment of all 15 human kallikreins and bovine  $\alpha$ -chymotrypsin (Figure 1A) shows that the region spanning the S1 pocket contains a number of highly conserved residues that are critical for the structural integrity of the pocket and indirectly responsible for the maintenance of enzymatic activity. Specifically, residues such as Cys<sup>191</sup>, Cys<sup>220</sup>, Pro<sup>225</sup>, and Ser<sup>214</sup> form crucial elements of the architecture surrounding the S1 pocket (22). Conversely, the variable regions of residues 183–190 and 221–224 within a given serine protease dictate the specificity of substrates and inhibitors for the individual protease.

For all serine proteases, substrate and inhibitor recognition is mainly governed by the binding of the P1 residue to the S1 pocket of the enzyme (Figure 1B). The amino acid residue at the bottom of the S1 pocket is therefore the key determinant for the P1 preference. For the majority of the kallikreins, this residue is aspartic acid. Thus, the majority of kallikreins exhibit trypsin-like specificity, cleaving after basic amino acids such as arginine and lysine. In contrast, for PSA the residue at the bottom of the pocket is serine (i.e., Ser<sup>189</sup>). Chymotrypsin also has serine in this position, and like PSA, it cleaves after hydrophobic residues. Two other kallikreins also have a unique (i.e., non-aspartic acid) amino acid in the S1 pocket with KLK7 having asparagine and KLK9 having glycine at this position.

The Ser<sup>189</sup> residue in the PSA S1 pocket is flanked by the polar side chains of Ser<sup>226</sup> and Thr<sup>190</sup> (Figure 1B). The alignment of the polar hydroxyl moieties of these residues

at the bottom of the pocket results in a cavity that is polar at the bottom but hydrophobic on the sides due to the aliphatic parts of the side chains forming the walls of the cavity. As shown in Figure 1B, the aromatic ring of a P1 tyrosine residue is optimally sandwiched between the hydrophobic cavity walls while making a hydrogen bond with the backbone carbonyl of the Ser<sup>217</sup> residue via its hydroxyl moiety. Thus, a residue like tyrosine with a medium-sized hydrophobic side chain and a polar phenolic group is ideal for binding at the S1 pocket of PSA. Other medium-sized hydrophobic side chains such as leucine and norleucine can also interact favorably with this pocket. The other residues, Thr<sup>190</sup>, Thr<sup>213</sup>, and Ser<sup>226</sup>, in the vicinity of the 189-position in the PSA protein are also responsible for the subtle variations in the polarity and hydrophobic character of the S1 binding site. These residues produce a pocket that is truly unique in its binding characteristics (23).

With the crystal structure of PSA now available, it is possible to utilize the true structural information of PSA to decipher the molecular details of the interactions in the S1 pocket. This information can be used to design more specific and potent inhibitors of PSA. Toward this end, we have employed the GOLD docking methodology to explore the binding modes of the 17 synthesized peptide aldehyde inhibitors of PSA described above. The inhibitors with the highest potencies (i.e., **16** and **17**) also had the highest GOLD scores of 38.84 and 39.66 (Table 1). Conversely, the compounds with the lowest inhibitory potencies (i.e., **12** and **15**) ranked in the bottom tier in terms of their GOLD scores.

Table 2: Specificity of Six Peptide Aldehydes for PSA versus Chymotrypsin and Corresponding GOLD Scores for Each Protease

compd	PSA $K_i$ ( $\mu$ M) <sup>a</sup>	Chy/PSA ratio <sup>b</sup>	Chy $K_i$ ( $\mu$ M) <sup>a</sup>	PSA GOLD score	Chy GOLD score
<b>1</b>	45.21 $\pm$ 3.89	>1000	>22	33.44	16.53
<b>2</b>	2.53 $\pm$ 0.13	>100	>40	30.66	14.27
<b>4</b>	0.91 $\pm$ 0.06	>100	>110	29.54	19.25
<b>9</b>	3.84 $\pm$ 0.21	>100	>26	34.78	23.07
<b>16</b>	0.57 $\pm$ 0.04	0.62 $\pm$ 0.05	1.08	38.84	28.38
<b>17</b>	0.37 $\pm$ 0.02	0.29 $\pm$ 0.03	0.78	39.66	28.86

<sup>a</sup> Value reported is for  $n = 3$  ( $\pm$ SE). <sup>b</sup> PSA selectivity in terms of (chymotrypsin  $K_i$ )/(PSA  $K_i$ ).

Overall, for 17 of the peptide aldehyde inhibitors, the  $K_i$  values, when converted to their free energy values via log transformations, correlate modestly with the GOLD score as indicated by the correlation coefficient of 0.64 (Supporting Information). The absence of a high correlation between  $K_i$  values and the GOLD scores can be explained by the fact that the strength of binding in the S1 pocket as quantified by the GOLD score does not take into account the entropic and solvation contribution of binding. Also, protein breathing at the binding site is not allowed during GOLD docking, resulting in possible inaccuracies in the exact magnitude of the energetic interactions. While it is not possible to use the GOLD score solely to differentiate between inhibitors with  $K_i$  values in a narrow range, the scores can be used to bucket the inhibitors into three different categories: those inhibitors with a GOLD score in the range of 16–24, 26–36, and  $\geq 38$  with  $K_i$  values typically in the range of 100, 10–100, and  $\sim 1$   $\mu$ M, respectively.

**Effects of PSA Inhibitors on Chymotrypsin Activity.** The results obtained from the PSA inhibitor studies and the corresponding docking analysis helped to define the key interactions between the amino acids in the S1 pocket of PSA and the substituents in the P1 position of the inhibitors. In order to better understand and define the unique substrate specificity for PSA compared to chymotrypsin, the PSA peptide aldehyde inhibitors were tested for their ability to inhibit chymotrypsin. The full-length glutamine aldehyde **1** had no ability to inhibit chymotrypsin with a  $K_i$  for

chymotrypsin  $>1000$   $\mu$ M (Table 2). Likewise, the noncyclizable  $\gamma$ -*N,N*-dimethylglutamine derivative **2** did not inhibit chymotrypsin to any degree nor did the glutamine isostere **4**. Both had  $K_i$  values for chymotrypsin above 100  $\mu$ M. The methionine peptide aldehyde **9** showed a similar pattern, being highly specific for PSA and not for chymotrypsin with a chymotrypsin  $K_i$  value above 100  $\mu$ M. As expected, compounds **16** and **17**, which are peptide aldehydes with hydrophobic P1 residues, were almost equally potent for PSA and chymotrypsin.

To better understand the structural differences between these two proteases that underlie the differences in inhibitory potency, we used a similar GOLD docking methodology to compare the binding modes of six peptide aldehyde inhibitors for both PSA and chymotrypsin. Table 2 presents the respective  $K_i$  values and the GOLD scores of these compounds when their P1 side chain was docked in the S1 pocket of either protease. Remarkably, the difference in the potency of **1**, **2**, **4**, and **9** against PSA vs chymotrypsin was consistent with the respective differences in GOLD scores. A drastic difference was especially notable for compounds **1**, **2**, and **4**. These compounds, all highly specific for PSA, had low GOLD scores for chymotrypsin (16.53, 14.27, 19.25) and correspondingly high  $K_i$  values ( $>100$   $\mu$ M). Similarly, **16** and **17** had high GOLD scores for PSA and chymotrypsin and were equally potent inhibitors of both proteases.

## DISCUSSION

These results expand upon our previous study in which we defined the potency of a series of peptidyl boronic acid based inhibitors of PSA and identified an inhibitor, Z-SSKL(boro)L, that had a  $K_i$  for PSA of 65 nM (14). This lead inhibitor had an  $\sim 65$ -fold higher  $K_i$  for chymotrypsin, even though it contained a hydrophobic leucine in the P1 position. For this earlier study, we employed a three-dimensional structural model of PSA that was developed based on the crystal structure of porcine kallikrein (PDB code 2PKA) and the human tissue kallikrein KLK1 (PDB code 1SPJ) (14, 18). This model was used to characterize the binding interactions between this “lead” inhibitor and

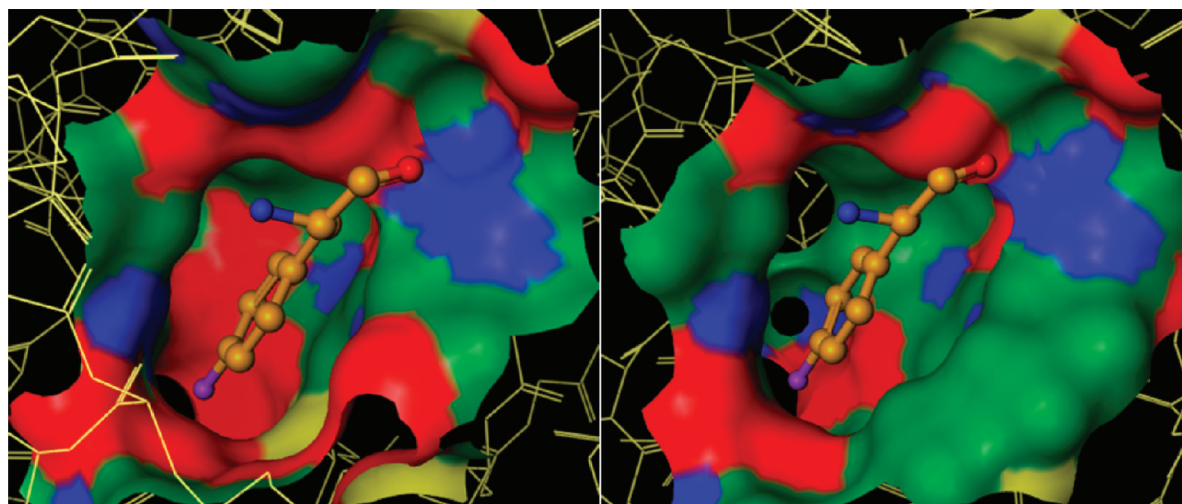


FIGURE 2: Surface representation of the S1 pocket of PSA (left) and bovine  $\alpha$ -chymotrypsin (right). The P1 tyrosine residue is shown as a yellow ball-and-stick model. The polar hydroxyl moiety of the bound residue is depicted in purple. Surface colors represent the following motifs: green is a mostly hydrophobic surface composed of aromatic and/or aliphatic carbons, red is a surface formed by polar oxygen atoms (backbone and side chain), blue is a polar surface formed by nitrogen atoms, and yellow is a surface formed by cysteine disulfide bonds.

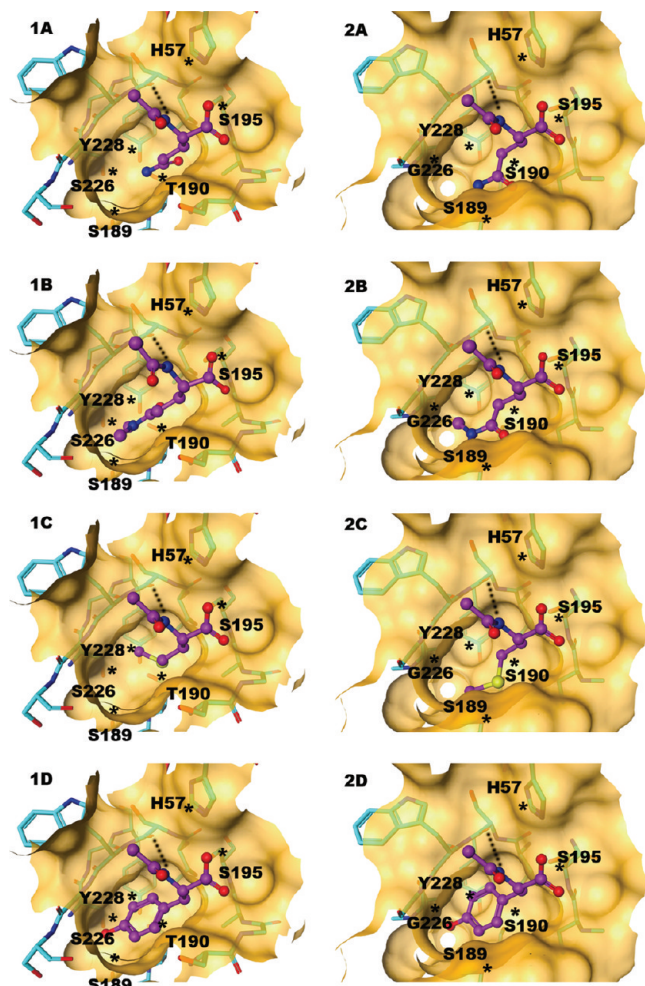


FIGURE 3: Comparison between the P1 side chains of selected inhibitors docked in the S1 pocket of PSA and chymotrypsin, respectively. Panels on the left side: 1A–1D present the binding modes of inhibitors **1**, **2**, **9**, and **17** in the catalytic pocket of PSA. Panels on the right side: 2A–2D present the same for inhibitors **1**, **2**, **9**, and **17** in the catalytic pocket of chymotrypsin. Inhibitor backbones are depicted in purple. The location of key protease residues relative to the docked inhibitors is pinpointed by an asterisk. The nitrogen and oxygen heavy atoms of inhibitors are delineated by blue and red solid spheres.

the PSA catalytic site. Subsequently, the crystal structure of PSA bound to an antibody has been published. In the current study, we revised our earlier model based on the published crystal structure and used this more refined model to characterize peptide aldehyde inhibitor binding to the S1 pocket of PSA.

PSA and chymotrypsin have previously been considered similar in their P1 specificity because of the presence of Ser<sup>189</sup> at the bottom of the S1 pocket in both proteases. For this reason, when describing its enzymatic activity, PSA is typically described as a “chymotrypsin-like protease”. However, here we document the important differences in the physical and electrostatic characteristics of the S1 pocket of these two serine proteases. In the case of PSA, the presence of the polar hydroxyl side chain of Ser<sup>189</sup>, Thr<sup>190</sup>, Thr<sup>213</sup>, and Ser<sup>226</sup> provides a noticeable polar character to its shallow bottom (red region in Figure 2). In contrast, the presence of Val<sup>213</sup> and Gly<sup>226</sup> produces a less polar and more spacious bottom of the S1 cavity of chymotrypsin (Figure 2). These structural differences in the S1 pocket underlie the significant

differences in  $K_i$  values observed for PSA compared to chymotrypsin for many of the inhibitors analyzed in this study.

The preference for glutamine in the P1 position is a unique characteristic of PSA that is not shared by other mammalian serine proteases (11, 12). In contrast, chymotrypsin has no ability to cleave after glutamine (13). As described here, chymotrypsin is also not inhibited appreciably by aldehyde inhibitors containing glutamine or glutamine analogues in the P1 position. A comparative analysis of the binding modes of inhibitor **1** (glutamine at the P1 position) docked in the S1 pocket of PSA and chymotrypsin, respectively (Figure 3: 1A and 2A), reveals drastic differences in orientation of the glutamine side chain that underlies the marked difference in  $K_i$  values for this inhibitor for these two proteases. In the PSA-docked conformation, the amide side chain of glutamine formed a hydrogen bond with Thr<sup>190</sup>. This hydrogen bond was not observed in the chymotrypsin-docked conformation since chymotrypsin has a serine residue instead of threonine at the 190-position. The amide group of **1** adopts a different orientation in which the carbonyl moiety is pointing toward Met<sup>192</sup>. This conformation might result in the loss of a hydrogen bond and suboptimal hydrophobic interactions between the aliphatic portion of the P1 side chain and S1 pocket hydrophobic surface of chymotrypsin.

Analysis of the binding modes of other inhibitors further highlights the structural differences between the two proteases. The side chain of inhibitor **2** (Figure 3: 1B and 2B) docked in the S1 pocket with PSA and chymotrypsin showed many similarities with that of inhibitor **1**. The orientation of **2** inside of PSA is similar to that of **1** in spite of the fact that the nitrogen of the tertiary amine moiety lacks the ability to function as a hydrogen bond donor. In chymotrypsin, this conformation can result in suboptimal hydrophobic interactions and steric clashes with the S1 pocket corresponding to its weak inhibitory potency. A similar rationale can be applied for inhibitor **9** (methionine at the P1 position) that also docks in a drastically different conformation. In the catalytic pocket of PSA (Figure 3: 1C), the terminal C $\epsilon$  atom of **9** is oriented toward Tyr<sup>228</sup> whereas the same atom is positioned in the vicinity of Ser<sup>189</sup> in the catalytic pocket of chymotrypsin (Figure 3: 2C). In contrast to inhibitor **9**, the tyrosine moiety of inhibitor **17** adopts similar conformations (Figure 3: 1D and 2D) in the S1 pocket of both PSA and chymotrypsin. This is consistent with the equal inhibitor potency of this inhibitor against both PSA and chymotrypsin. It is interesting to note that the tyrosine hydroxyl moiety makes a tight hydrogen bond with the Ser<sup>226</sup> side chain in the PSA catalytic pocket. Since serine at the 226-position is replaced by glycine in chymotrypsin, the hydrogen bond acceptor is supplied by the backbone carbonyl of the Ser<sup>190</sup> residue.

In conclusion, the results presented here highlight the unique characteristics of the S1 specificity pocket of PSA that differentiate it from chymotrypsin and other members of the kallikrein family of serine proteases. Based on these unique characteristics, these results also document that the development of a highly specific inhibitor of PSA is feasible. In this regard, we are currently pursuing a strategy to design boronic acid based inhibitors of PSA that can be used to selectively target therapeutic agents to prostate cancer sites. While the synthesis of a glutamine boronic acid analogue is

not feasible, it is possible to synthesize boronic acid derivatives of compounds **4** and **5**. Boronic acid derivatives of these compounds, as well as derivatives of phenylalanine and tyrosine, are currently being synthesized in our laboratory, and inhibitors based on these derivatives will be tested for their ability to inhibit PSA selectively compared to other proteases. In addition, the exclusive production of PSA by prostate cancers suggests that novel agents for imaging prostate cancer within bone and soft tissue sites can be developed through the incorporation of imaging modalities such as chelating groups into the structure of these PSA-specific inhibitors.

## SUPPORTING INFORMATION AVAILABLE

A more detailed description of the chemical syntheses described in this report including NMR spectra and mass spectroscopic analyses, data for all of the components used to calculate Gold scores for the top docking pose for each inhibitor and data showing the correlation between the Gold score and the  $K_i$  values for each inhibitor, and a linear plot of  $\nu_0/\nu_i - 1$  vs  $[I]$  and a Hanes–Woelf plot for the best PSA inhibitor at different concentrations. This material is available free of charge via the Internet at <http://pubs.acs.org>.

## REFERENCES

1. Yousef, G. M., and Diamandis, E. P. (2003) An overview of the kallikrein gene families in humans and other species: emerging candidate tumour markers. *Clin. Biochem.* **36**, 443–452.
2. Williams, S. A., Singh, P., Isaacs, J. T., and Denmeade, S. R. (2007) Does PSA play a role as a promoting agent during the initiation and/or progression of prostate cancer? *Prostate* **67**, 312–329.
3. Lilja, H. (1985) A kallikrein-like serine protease in prostatic fluid cleaves the predominant seminal vesicle protein. *J. Clin. Invest.* **76**, 1899–1903.
4. Lilja, H., Abrahamsson, P. A., and Lundwall, A. (1989) Semenogelin, the predominant protein in human semen. Primary structure and identification of closely related proteins in the male accessory sex glands and on the spermatozoa. *J. Biol. Chem.* **264**, 1894–1900.
5. Malm, J., Hellman, J., Hogg, P., and Lilja, H. (2000) Enzymatic action of prostate-specific antigen (PSA or hK3): substrate specificity and regulation by  $Zn^{2+}$ , a tight-binding inhibitor. *Prostate* **45**, 132–139.
6. Cohen, P., Graves, H. C., Peehl, D. M., Kamarei, M., Giudice, L. C., and Rosenfeld, R. G. (1992) Prostate-specific antigen (PSA) is an insulin-like growth factor binding protein-3 protease found in seminal plasma. *J. Clin. Endocrinol. Metab.* **75**, 1046–1053.
7. Iwamura, M., Hellman, J., Cockett, A. T., Lilja, H., and Gershagen, S. (1996) Alteration of the hormonal bioactivity of parathyroid hormone-related protein (PTHrP) as a result of limited proteolysis by prostate-specific antigen. *Urology* **48**, 317–325.
8. Cramer, S. D., Chen, Z., and Peehl, D. M. (1996) Prostate specific antigen cleaves parathyroid hormone-related protein in the PTH-like domain: inactivation of PTHrP-stimulated cAMP accumulation in mouse osteoblasts. *J. Urol.* **156**, 526–531.
9. Dallas, S. L., Zhao, S., Cramer, S. D., Chen, Z., Peehl, D. M., and Bonewald, L. F. (2005) Preferential production of latent transforming growth factor-2 by primary prostatic epithelial cells and its activation by prostate-specific antigen. *J. Cell. Physiol.* **202**, 361–370.
10. Lilja, H., Piironen, T. P., Rittenhouse, H. G., Mikolajczyk, S. D., and Slawin, K. M. (2000) *Comprehensive Textbook of Genitourinary Oncology*, pp 638–650, Lippincott Williams and Wilkins, Philadelphia.
11. Dragovich, P. S., Prins, T. J., Zhou, R., Webber, S. E., Marakovits, J. T., Fuhrman, S. A., Patrick, A. K., Matthews, D. A., Lee, C. A., Ford, C. E., Burke, B. J., Rejto, P. A., Hendrickson, T. F., Tuntland, T., Brown, E. L., Meador, J. W., Ferre, R. A., Harr, J. E., Kosa, M. B., and Worland, S. T. (1999) Tripeptide aldehyde inhibitors of human rhinovirus 3C protease: design, synthesis, biological evaluation, and co-crystal structure solution of P1 glutamine isosteric replacements. *J. Med. Chem.* **42**, 1213–1224.
12. Helmerhorst, E. J., Sun, X., Salih, E., and Oppenheim, F. G. (2008) Identification of lys-pro-gln as a novel cleavage site specificity of saliva-associated proteases. *J. Biol. Chem.* **283**, 19957–19966.
13. Denmeade, S. R., Lou, W., Malm, J., Lovgren, J., Lilja, H., and Isaacs, J. T. (1997) Specific and efficient peptide substrates for assaying the proteolytic activity of prostate-specific antigen. *Cancer Res.* **57**, 4924–4930.
14. LeBeau, A. M., Singh, P., Isaacs, J. T., and Denmeade, S. R. (2008) Potent and selective peptidyl boronic acid inhibitors of the serine protease prostate-specific antigen. *Chem. Biol.* **15**, 665–674.
15. Malcolm, B. A., Lowe, C., Shechosky, S., McKay, R. T., Yang, C. C., Shah, V. J., Simon, R. J., Vederas, J. C., and Santi, D. V. (1995) Peptide aldehyde inhibitors of hepatitis A virus 3C proteinase. *Biochemistry* **34**, 8172–8179.
16. Webber, S. E., Okano, K., Little, T. L., Reich, S. H., Xin, Y., Fuhrman, S. A., Matthews, D. A., Love, R. A., Hendrickson, T. F., and Patrick, A. K. (1998) Tripeptide aldehyde inhibitors of human rhinovirus 3C protease: design, synthesis, biological evaluation, and cocrystal structure solution of P1 glutamine isosteric replacements. *J. Med. Chem.* **41**, 2786–2805.
17. Kappel, J. C., and Barany, G. (2005) Backbone amide linker (BAL) strategy for N-9-fluorenylmethoxycarbonyl (Fmoc) solid-phase synthesis of peptide aldehydes. *J. Peptide Sci.* **11**, 525–535.
18. Singh, P., Williams, S. A., Shah, M. H., Lectka, T., Pritchard, G. J., Isaacs, J. T., and Denmeade, S. R. (2008) Mechanistic insights into the inhibition of prostate-specific antigen by  $\beta$ -lactam class compounds. *Proteins* **70**, 1416–1428.
19. Salvesen, G. S., and Nagase, N. (2001) *Proteolytic Enzymes* (Benyon, R., and Bond, J. S., Eds.) 2nd ed., pp 131–147, Oxford University Press, Oxford.
20. Menez, R., Michel, S., Muller, B. H., Bossus, M., Ducancel, F., Jolivet-Reynaud, C., and Stura, E. A. (2008) Crystal structure of a ternary complex between human prostate-specific antigen, its substrate acyl intermediate and an activating antibody. *J. Mol. Biol.* **376**, 1021–1033.
21. Debela, M., Magdolen, V., Schechter, N., Valachova, M., Lottspeich, F., Craik, C. S., Choe, Y., Bode, W., and Goettig, P. (2006) Specificity profiling of seven human tissue kallikreins reveals individual subsite preferences. *J. Biol. Chem.* **281**, 25678–25688.
22. Krem, M. M., Prasad, S., and Di Cera, E. (2002) Ser214 is crucial for substrate binding to serine proteases. *J. Biol. Chem.* **277**, 40260–40264.
23. Guinto, E. R., Caccia, S., Rose, T., Futterer, K., Waksman, G., and Di Cera, E. (1999) Unexpected crucial role of residue 225 in serine proteases. *Proc. Natl. Acad. Sci. U.S.A.* **96**, 1852–1857.

BI9001858